ISSN 1995-0780, Nanotechnologies in Russia, 2014, Vol. 9, Nos. 3–4, pp. 168–174. © Pleiades Publishing, Ltd., 2014.
Original Russian Text © Ya.I. Odarchenko, D.V. Anokhin, A.A. Piryazev, E.M. Antipov, V.A. Gerasin, D.I. Mendeleev, V.V. Bazarkina, A.I. Smirnov, D.S. Krivezhenko, A.Yu. Chumachenko, D.A. Ivanov, 2014, published in Rossiiskie Nanotekhnologii, 2014, Vol. 9, Nos. 3–4.

Investigation into the Morphology of Aliphatic Segmented Block Copolymers with Controlled Thickness of Crystals

Ya. I. Odarchenko[a], D. V. Anokhin[b], A. A. Piryazev[b], E. M. Antipov[c], V. A. Gerasin[c], D. I. Mendeleev[c], V. V. Bazarkina[d], A. I. Smirnov[d], D. S. Krivezhenko[d], A. Yu. Chumachenko[d], and D. A. Ivanov[a, b]

[a] *Institut de Sciences des Materiaux de Mulhouse, CNRS UMR 7361, 15, Jean Starcky, F-68057, Mulhouse, France*
[b] *Faculty of Fundamental Physical and Chemical Engineering, Moscow State University, Moscow, 119991 Russia*
[c] *Topchiev Institute of Petrochemical Synthesis, Russian Academy of Sciences, Leninskii pr. 29, Moscow, 119991 Russia*
[d] *Novosibirsk State Technical University, pr. K. Marksa 20, Novosibirsk, 630073 Russia*
e-mail: dimitri.ivanov@uha.fr

Received August 27, 2013; in final form, December 12, 2013

Abstract—In the present paper, aliphatic thermoelastoplastics, consisting of alternating segments of polytetrahydrofuran and monodisperse segments of glycine and β-alanine bisoxalamides, are studied. Phase transitions and the orientation of crystals are determined by experiments using X-ray structural analysis during the drawing process in situ. Two types of morphology have been revealed. Fibrillar crystals with chains oriented perpendicularly to the drawing direction are formed at low draw ratio values. At high deformation degrees, a fracture of large crystals and a reorientation of polymer chains along the drawing direction are observed. It is shown that the thickness of the hard block crystals is constant and independent of the sample thermal prehistory. The tilting angle of bisoxalamide chains is determined using four-spot small-angle patterns. It turns out that in the case of glycine the tilting angle is rather small (~5–15°), while for alanine it reaches 24°. The flexible block crystallization during the drawing process at room temperature was found regardless of the block length. The surface free energy of hard block crystals proved to be rather low (~18 erg/cm^2), which is probably due to the entropic contribution from flexible blocks.

DOI: 10.1134/S1995078014020104

INTRODUCTION

The latest advances in the field of creating thermoelastoplastics (TEPs) have caused interest in investigations of their structure and properties [1–3]. As a rule, these materials possess a phase-separated morphology in the temperature range of their application, and the morphology depends on their chemical structure, molecular weight, and polydispersity of both soft and hard blocks, as well as on their thermal history. A special class of TEP is presented by segmented block-copolymers with hard blocks of exactly identical lengths, which demonstrate the ability to quickly and completely crystallize. As a result, fibrillar crystals are formed consisting of hard segments surrounded by an amorphous matrix of soft segments [4, 5]. It is important to note that experimental methods such as AFM and DSC reveal a precise monodispersity of crystals in their thickness, which is uncharacteristic of partially crystalline polymers [6–9]. The formation of such crystals monodisperse in their thickness in TEP based on segmented block copolymers is their important advantage, since it allows a partially crystalline morphology, weakly dependent on the forming conditions, to be obtained.

Structural transformations of TEPs upon their drawing were intensively studied with the use of various methods. It has been established that two main stages of the structural reorganization of copolymers are observed upon their deformation [4, 6]. At draw ratio values below the yield point, hard segments of chains in crystals are predominantly oriented perpendicularly to the drawing direction. Above the yield point, a fragmentation of crystals occurs, and, as a result, hard segments become oriented along the draw axis. At high deformations, lamellae are fractured and form strongly loaded nanofibrils consisting of alternating hard and crystallized soft segments [10, 11]. Experiments on small-angle X-ray diffraction showed the presence of a four-spot pattern in relatively early stages of the drawing (about 5–150%), indicating the formation of a morphology with tilted crystals of hard blocks caused by a high characteristic ratio of their sides [10, 12]. For classical polyolefins, this phenomenon is explained by a tilt of folded chains relative to the surface of lamellae [13, 14]. For the first time, the tilting angle of chains in polyethylene (PE) φ was calculated by Peterlin from the difference in large periods before and after the deformation [13]. Later, the value φ was determined in experiments on X-ray and electron diffraction [15, 16]. Finally, our research group managed to obtain a precise tilting angle value for chains in bulk PE crystals, 35°, using the microfocus

X-ray diffraction method [17]. To the best of our knowledge, the topic of chain tilting in crystals of phase-separated block-copolymers has not yet been thoroughly discussed in literature. This fact is due to the complicated character of studies of chain packing in nanometer-scale fibrillar crystals attached chemically to flexible blocks of an amorphous matrix [5]. Despite the complete crystallization of a hard block (the degree of crystallinity reaches 100%), its weight fraction in TEPs is, as a rule, low (25% at most), and this circumstance restricts the application of classical structural methods [14].

In the present work, a polymer system with a crystal structure defined in the synthesis stage is studied. To investigate the deformation behavior of poly(ether-ether amides) (PEEA) under examination, X-ray measurements were performed in situ in the drawing process of copolymer films. In particular, the orientation of crystals and phase transitions, occurring in both blocks, were studied. The morphology of oriented segmented copolymers was also studied by the method of high-temperature small-angle X-ray scattering with the use of a synchrotron radiation source. In the present paper, the roles of the thickness and monodispersity of fibrillar crystals formed of hard blocks, as well as the low surface energy values calculated for these crystals, are discussed.

SAMPLES AND METHODS OF INVESTIGATION

The hard block of segmented PEEA consists of bisoxalamide with glycine end groups. The soft block is represented by polytetrahydrofuran (PTHF) of variable molecular weight. The samples are denoted as presented below (Scheme 1).

The synthesis of samples is described in detail in previous publications [18]. In scheme 1, n is the average molecular weight of PTHF (g/mol). The samples under investigation in the form of yellow transparent elastic films were prepared by melt extrusion followed by further cooling upon either quenching in a water/ice mixture or slow cooling from the melt with the rate 5°C/min.

Experiments on wide-angle (WAXS) and small-angle X-ray scattering (SAXS) were carried out on the line BM26 of the European center of synchrotron radiation (Grenoble, France) with the use of the wavelength 1.04 Å. For the measurements, two-dimensional FreLon detectors for WAXS and Pilatus 1M detectors for SAXS were used. The measured range of the modulus of the reciprocal space vector s ($s = 2\sin\theta/\lambda$, where θ is Bragg angle) was from 0.01 to 0.5 $Å^{-1}$. The scattering vector module in both configurations was calibrated by several diffraction orders of silver behenate. The diffraction signal was recorded in the transmission mode. In high-temperature experiments, the sample temperature was maintained with an accuracy of ±2°C. The crystal thicknesses (L_c) ðwere calculated from the scattering profile form obtained via the integration of two-dimensional diffraction patterns using the following expression:

$$I(s) \propto A + \frac{B}{s^n}\left(\frac{\sin(\pi s L_c)}{(\pi s L_c)}\right)^2. \quad (1)$$

Films used in experiments on their uniaxial drawing were cut out of the cast films ($3 \times 10 \times 1$ mm^3). The experiments were performed using a Linkam TST 350 specialized deformation attachment. In the experiments, three different deformation rates were used (20, 30, and 60 μm/s).

The size of crystallites was estimated from a one-dimensional WAXS profile via the Selyakov–Scherrer formula:

$$l_{hkl} = \frac{0.94\lambda}{\Delta\cos\vartheta}. \quad (2)$$

Experiments on transmission electron microscopy (TEM) were conducted on a Philips CM200 microscope with the working frequency 200 keV. Carbon was used for the calibration of electron diffraction patterns.

Samples were prepared via precipitation from toluene onto a slide glass followed by the detachment of a sample in a 1% aqueous solution of hydrofluoric acid. Samples were placed onto TEM grids from the solution.

RESULTS AND DISCUSSION

Using the results on X-ray diffraction and IR spectroscopy, it was shown that the crystal structure of hard segments in block-copolymers is close to that of the corresponding monomers [5]. Thus, it was important to investigate the structure of monomers forming hard segments. Needlelike single crystals of the monomer Gly-$Oxa_2$6-Gly (the hard block of samples 3-5) were prepared for TEM experiments. An example of X-ray diffraction pattern obtained for Gly-$Oxa_2$6-Gly is presented in Fig. 1a. The observed diffraction peaks are assigned to the diffraction zone [02-1]. With the use of IR spectroscopy and X-ray diffraction, it was revealed that the direction of hydrogen bonds is parallel to the crystal ***a*** (Fig. 1b) [5]. In the case of polymers, the direction of hydrogen bonds is determined by the number of carbon atoms between oxalamide groups [19, 20, 21]. One direction is observed for an even number of atoms in the spacer, while for an odd number two directions are observed. Since all monomers in our work have even numbers of carbon atoms in the spacer, the results agree with the literature data. The needle growth direction corresponds to the crystallographic direction {100}, as is seen from Fig. 1c.

The indexing of electron diffraction patterns, corresponding to several diffraction zones, made it possible to determine that the cell of the monomer Gly-$Oxa_2$6-Gly is of the monoclinic type (symmetry C_2)

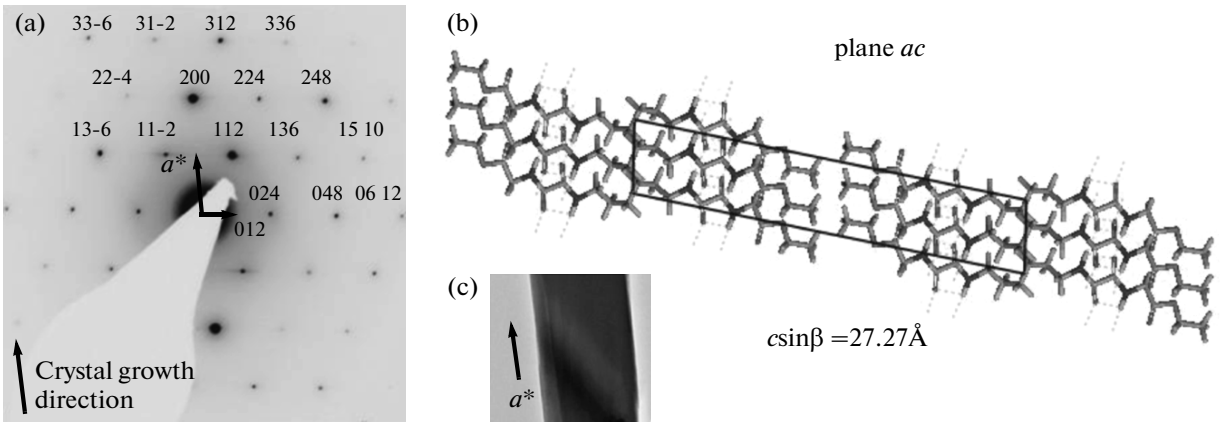

Fig. 1. Electron diffraction pattern for the diffraction zone [0-21] (a) and TEM image of a needlelike crystal (c); the growth direction is indicated by the arrow. Monomer Gly-Oxa$_2$6-Gly cell model. Hydrogen bonds are shown by dashed lines (b).

and has the following parameters: a = 5.09 Å, b = 10.88 Å, c = 27.73 Å, and β = 79.6° (Table 1). The calculated value of the interchain distance along the direction of hydrogen bonds corresponds to that characteristic of nylon 6.2 [21]. The **ac** projection of the Gly-Oxa$_2$6-Gly cell model is shown in Fig. 1c. The elementary cell contains two molecules, the neighboring molecules forming layers in the **ac** plane connected by hydrogen bonds.

For a study of structural changes upon the deformation of segmented PEEA films, in situ X-ray diffraction experiments were conducted directly during the drawing process. The obtained two-dimensional diffraction patterns of sample **5** are presented in Fig. 2. As is seen from Fig. 2a, the original film is fully isotropic with an amorphous halo at ca. 4.4 Å and crystalline 200 and 220 peaks (the spacings 2.48 Å, 2.30 Å, respectively) of the monoclinic bisoxalamide lattice. A schematic model of a nonoriented morphology, consisting of fibrillar crystals immersed into an amorphous matrix of soft blocks, is shown in Fig. 3a [5, 18]. At 50% deformation, a weak anisotropy is observed in samples, being revealed through an orientation of peaks corresponding to direction {100} along hydrogen bonds, in the meridian region (Fig. 2b). Thus, sheets formed by hydrogen bonds are oriented parallel to the drawing axis (Fig. 3b). A similar orientation of crystallites with a high characteristic ration was observed earlier at small deformations by Niesten [6] and Versteegen [4] using IR spectroscopy. It should be noted that no crystal phase of the soft block is formed at low draw ratios. Above the yield point (for sample **5** it is about 100% [18]), spotlike crystalline reflections of bisoxalamide at the meridian and a diffuse layer line, corresponding to the PTHF crystal structure, appear. The latter arises due to orientational crystallization [6, 10, 12]. By analyzing periodicity along axis **c**, it was established that polytetrahydrofuran chains are oriented parallel to the drawing direction (Fig. 3c). Upon further deformation (above 300%), PTHF crystalline peaks become more intense and better oriented (Fig. 2d). Details of the formation of the soft block crystal phase are described below. It is seen form Fig. 2d that crystalline peaks of hard and soft blocks overlap. To get rid of this problem, films were heated above the PTHF melting temperature up to 80°C [6] (Fig. 4). It is seen in that case that 200 and 220 peaks are arranged at the equator, pointing to the fact that the **c*** axis of the cell of bisoxalamide is predominantly oriented along the drawing axis (Fig. 3c). Thus, at high draw ratios, both hard and soft segments form micellar crystals with chains oriented parallel to

Table 1. Measured and calculated values of interplanar spacings for needlelike single crystals of the monomer Gly–Oxa$_2$6–Gly

h	k	l	d_{exp}, Å	d_{calc}, Å
0	2	4	4.25	4.25
0	4	8	2.13	2.13
0	6	12	1.43	1.42
1	3	–6	2.35	2.36
1	1	–2	4.12	4.12
1	1	2	4.5	4.54
1	3	6	2.62	2.60
1	5	10	1.67	1.67
2	6	12	1.3	1.30
2	4	8	1.72	1.72
2	2	4	2.27	2.27
2	0	0	2.51	2.50
2	2	–4	2.05	2.06
3	3	–6	1.37	1.37
3	1	–2	1.59	1.60
3	1	2	1.67	1.67
3	3	6	1.52	1.51

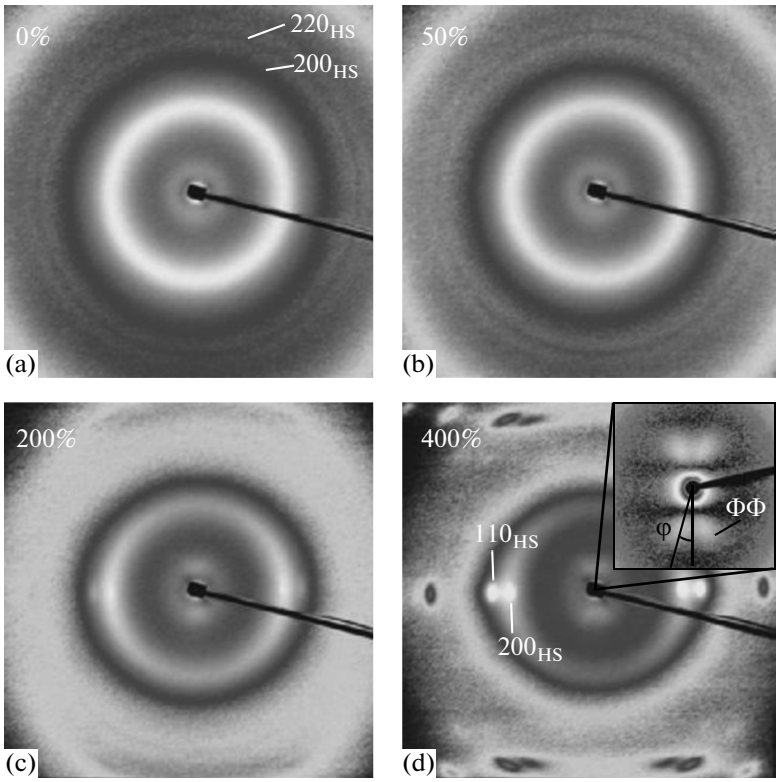

Fig. 2. WAXS diffraction patterns, corresponding to different deformation values for sample **3c** (a–d). The magnified region shows the presence of a four-spot pattern in the small-angle range (e). The drawing direction is vertical.

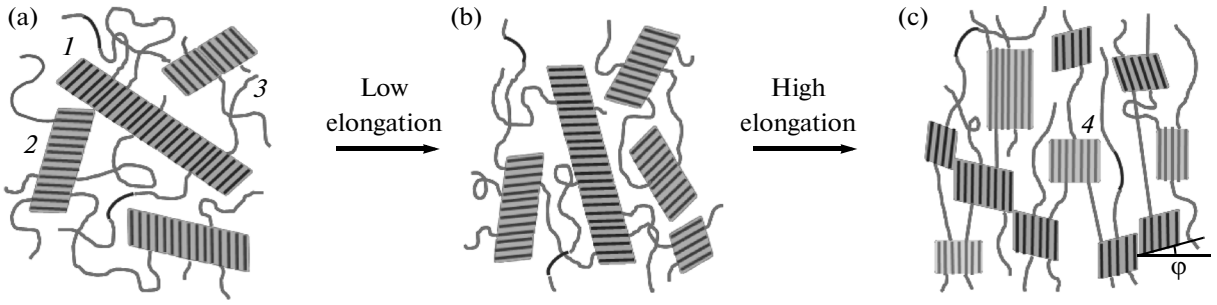

Fig. 3. Schematic model of structural changes in PEEA with hard blocks of the same length upon uniaxial deformation: (a) isotropic sample, (b) morphology below the yield point, and (c) morphology above the yield point. The denoted structural elements: (*1*) hard block, (*2*) crystals of the hard block, (*3*) soft block, (*4*) crystals of the soft block, and (φ) the tilting angle of the hard block chains. The drawing direction is vertical.

the drawing direction. This is in an agreement with the literature data, indicating that a fragmentation of crystals and their reorientation along the mechanical stress direction occur above the yield point [4, 6]. The presence of a crystal phase of bisoxalamide provides good mechanical properties of the films at ambient temperatures, causing the effect of physical nodes of an entanglement network. In the small-angle range, a signal is observed corresponding to the form factor of thickness-uniform crystals of bisoxalamide. An isotropic signal in the original films is transformed to a four-spot pattern at deformation above 300% (Fig. 2d). The formation of the tilted crystal morphology was earlier observed for block copolymers based on polyurethanes [10, 12], and its origin will be discussed below in more detail.

Morphology formation in highly oriented films is essentially affected by the soft block length. In Fig. 5a, diffraction patterns of PEEA samples strained up to 300% with hard block Gly-Oxa$_2$6-Gly and soft block of the length 1000 (**3**) and 2900 (**5**) g/mol, respectively, are presented. It is seen from these figures that 200 and 220 peaks of the monomer Gly-Oxa$_2$6-Gly cell are present on the diffraction patterns of samples **3** and **5**.

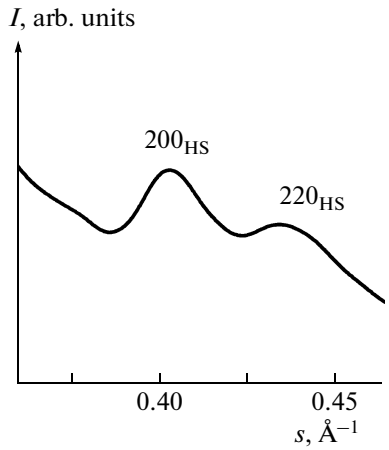

Fig. 4. Integrated one-dimensional diffraction pattern of sample 5 at 80°C with two peaks of the crystal lattice of bisoxalamide.

It is important to note that, in contrast to the monomer structure, where these reflections are weakly oriented and arranged at the meridian, well-oriented equatorial peaks are observed in segmented block-copolymers. These differences are explained by specific features of the orientation of nanocrystallites. As was mentioned above, after defragmentation, layers formed by hydrogen bonds in segmented PEEA crystals are oriented parallel to the drawing direction, forming characteristic micellar morphology. On the contrary, defragmentation is much more weakly pronounced in the monomer and, as a result, the crystal growth axis is aligned along the extrusion direction.

Crystallization upon drawing leads to the formation of a highly oriented monoclinic phase of PTHF described in literature [22]. It is important to note that the formation of the crystal PTHF phase in isotropic samples is observed only at the block length above 1000 g/mol and temperatures below room temperature (the temperatures are equal to −16.4 and 3°C for samples 4 and 5, respectively). Using high-temperature X-ray analysis, the soft block melting temperatures were compared in oriented and isotropic materials. It turned out that, for drawn samples, the value of T_m rises by more than 60°C. Similar results were obtained for TFT-PTHF block copolymers with the same hard block [6]. An increase in the soft block length also gives rise to a growth of the crystal size along the drawing direction. Thus, the correlation length calculated from the Selyakov–Scherrer equation for reflection 11-5 increases more than twice upon a lengthening of the PTHF block from 2000 (**4**) to 2900 (**5**). A hardening of the material upon its drawing due to the soft block crystallization brings about a 75% increase in the tensile strength and elongation at a break of sample **5** when compared to those of sample **4** [18].

SAXS measurements were used for to calculate the primary crystal parameters for the hard phase. As was expected, the thickness of bisoxalamide crystals (L_c) calculated from the position of the crystal form-factors is determined by the hard block length and is independent of the soft segment length (Table 2). One-dimensional SAXS curves of oriented samples **4**–**5** based on Gly-Oxa$_2$6-Gly are presented in Fig. 6. It is seen that the form-factor intensity decreases by more than twice with a growth of the hard block content from 10.5 to 25.4 wt %. The obtained L_c values are slightly lower than the parameter ***c*** projection onto the **b***$\mathbf{c}^*$ normal ($c^*\sin\beta$) corresponding to the interplanar spacing in the monomer lattice equal to 27.3 Å. The difference of 3.3 Å is due to the replacement of PTHF chains in the block copolymer for methyl end groups. It is seen from Table 2 that a slight thickening of bisoxalamide crystals is observed upon drawing. Supposing that this "thickening" depends on the spacer length, it may be concluded that alkyl chains between oxalamide monomers adopt a more extended conformation upon deformation.

Tilting angles of hard blocks with respect to the crystal surface were calculated from the azimuthal position of form-factor peaks in a four-spot SAXS pat-

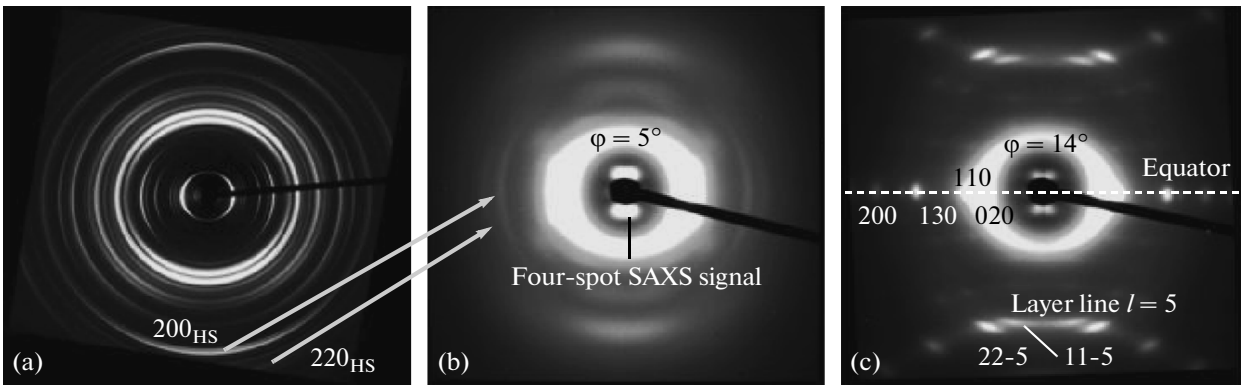

Fig. 5. Diffraction patterns of the monomer Gly-Oxa$_2$6-Gly (a) and block-copolymers on its basis with different soft block lengths: 1000 (b) and 2900 (c) g/mol.

Table 2. The long period (L_B), crystal thickness (L_c), and the amorphous layer thickness for isotropic and oriented PEEA block copolymers

Sample	Isotropic			Oriented			
	L_B, Å	L_c, Å	L_a, Å	L_B, Å	L_c, Å	L_a, Å	φ
1	49.8	14.3	35.5	50.9	16.3	34.6	~5–10
2	52.6	17.4	35.2	47.7	19.1	28.6	~5–10
3	57.5	24.0	33.5	57.3	27.7	29.6	~5–10
4	71.4	24.0	47.4	63.1	26.8	36.3	~5–10
5	79.0	24.0	55.0	78.4	26.8	51.6	~10–16

tern 5 (Fig. 5c). It was assumed that, since the **c*** axis of the cell of bisoxalamide is parallel to the draw axis, the chain tilting in the crystal is directly related to the tilting morphology of drawn films. It should be noted that, although the value φ changes from one sample to another, it stays constant above the yield point (Table 2). The φ values increase from 5 to 25° for samples with a long PTHF block.

Using the results on the crystal thickness L_c and melting temperature T_m, the surface energy of crystals σ_e was calculated via the Gibbs–Thompson equation:

$$T_m = T_m^0\left(1 - \frac{2\sigma_e}{\rho L_c \Delta H_f}\right), \quad (3)$$

where T_m° is the melting temperature of an infinitely thick crystal; ρ is the crystal density. The calculation showed that the value $\sigma_e = 18$ erg/cm^2 is identical for all block-copolymers. This value is noticeably lower when compared to common homopolymers [15]. Such behavior is related to the fact that the surface energy value is underestimated by the Gibbs–Thompson equation for needlelike crystals [5]. Similar results were obtained earlier for polyamide 6,6, and they were explained by a specific crystallization mechanism characteristic of nonpolymer materials [23]. In our case, a low surface energy value is probably due to the entropic contribution from the connecting flexible blocks, preventing a merge of growing hard block crystals with the formation of a classical lamellar structure.

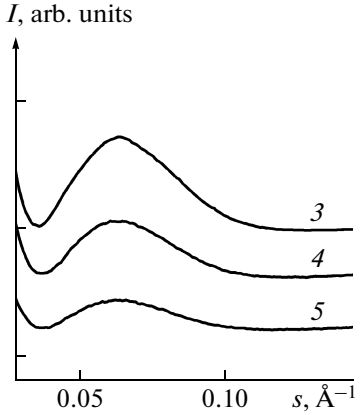

Fig. 6. SAXS curves of oriented samples **3**–**5**.

CONCLUSIONS

In the present work, new polymer TEP based on segmented PEEA with the crystal size determined precisely by the hard block chemical structure were investigated. A structural model of the monomer bisoxalamide was suggested based on an analysis of X-ray and electron diffraction data. It was revealed for block copolymers that the hard block structure matches the monomer structure with the direction of hydrogen bonds along the crystal **a** axis. The crystal thickness is strictly monodisperse, being determined in the stage of the block-copolymer synthesis. Also, in situ investigations of structural changes in the material upon its deformation were carried out. Two types of morphology were revealed. At low degrees of deformation, the physical network is destroyed, and this leads to the orientation of crystals along the drawing direction, polymer chains being perpendicular to the deformation axis. At high degrees of deformation, the fragmentation of bisoxalamide crystals occurs, being accompanied by the orientation of chains along the drawing direction. The tilting angles of chains relative to the crystal surface were calculated from four-spot diffraction patterns. Furthermore, it turned out that the surface energy values calculated from structural and thermophysical characteristics are nearly the same and rather low, which is due to geometrical restrictions during the crystallization process. The results are of importance for understanding the relationship between the crystal structure and the morphology of products with macroscopic properties of the new class of materials.

It should be noted that the developed materials are also of significant potential in the field of nanotechnology. Thus, compared to segmented copolymers on the basis of polyurethanes, segmented PEEA have a higher decomposition temperature, exceeding their melting temperature, and this fact makes their processing more adaptable to streamlined production. Moreover, PEEA copolymers are also characterized by a high chemical stability, flexibility at low temperatures, strength, and elasticity. These properties make them applicable for the production of foams, elastomer fibers, adhesives, fabrics, and sportswear. Furthermore, an interesting combination of structural parameters with excellent mechanical and surface properties makes it possible to use these copolymers for the production of hi-tech medical items, in particular, catheters.

ACKNOWLEDGMENTS

The authors are grateful to Niels Sijbrandi, Edwin Mes, Rene Broos, Georg Bar, and Pieter Dijkstra for providing samples and fruitful discussion. This work was supported by the Federal Target Program "Investigations Along Priority Directions of Development of Scientific and Technological Complex of Russia for 2007–2013 (state contract nos. 14.512.11.0010, 14.B37.21.0920 of September 10, 2012) and by the program of the Ministry of Education and Science of the Russian Federation for the support of leading scientists (state contract no. 11.31.0055G34 of October 19, 2011).

REFERENCES

1. R.-P. Eustache, *Handbook of Condensation Thermoplastic Elastomers,* Ed. by S. Fakirov (Wiley-VCH, Weinheim, 2005), Chapter 10, pp. 263–280.
2. S. A. Guelcher, Tissue Eng. Part B Rev. **14**, 3–17 (2008).
3. K. Kojio, M. Furukawa, S. Motokucho, M. Shimada, and M. Sakai, Macromolecules **42**, 8322–8327 (2009).
4. R. M. Versteegen, R. Kleppinger, R. P. Sijbesma, and E. Meijer, Macromolecules **39**, 772–783 (2006).
5. N. J. Sijbrandi, A. J. Kimenai, E. P. C. Mes, R. Broos, G. Bar, M. Rosenthal, Y. Odarchenko, D. A. Ivanov, P. J. Dijkstra, and J. Feijen, Macromolecules **45**, 3948–3961 (2012).
6. M. C. E. J. Niesten, S. Harkema, E. V. D. Heide, and R. J. Gaymans, Polymer **42**, 1131–1142 (2001).
7. C. De Ten Hove, J. Penelle, D. A. Ivanov, and A. M. Jonas, Nature Mater. **3**, 33–37 (2004).
8. D. A. Ivanov, G. Bar, M. Dosie, and M. H. J. Koch, Macromolecules **41**, 9224–9233 (2008).
9. D. A. Ivanov, S. Hocquet, M. Dosiére, and M. H. J. Koch, Eur. Phys. J. E: Soft Matter **13**, 363–378 (2004).
10. F. Yeh, B. S. Hsiao, B. B. Sauer, S. Michel, and H. W. Siesler, Macromolecules **36**, 1940–1954 (2003).
11. B. B. Sauer, R. S. Mclean, R. J. Gaymans, and M. C. J. E. Niesten, J. Polym. Sci.: Part B: Polym. Phys. **42**, 1783–1792 (2003).
12. R. Bonart, J. Macromolec. Sci. Part B **2**, 115–138 (1968).
13. A. Peterlin and F. J. Baltá-Calleja, Kolloid-Z. Z. Polym. **242**, 1093–1102 (1970).
14. A. Peterlin, J. Mater. Sci. **6**, 490–508 (1971).
15. S. Hocquet, M. Dosie, A. Thierry, B. Lotz, M. H. J. Koch, N. Dubreuil, D. A. Ivanov, and M. Dosière, Macromolecules **36**, 8376–8384 (2003).
16. S. Hocquet, M. Dosiere, and Y. Tanzawa, Macromolecules **35**, 5025–5033 (2002).
17. M. Rosenthal, G. Bar, M. Burghammer, and D. A. Ivanov, Angew. Chem. **123**, 9043–9047 (2011).
18. N. J. Sijbrandi, A. J. Kimenai, E. P. C. Mes, R. Broos, G. Bar, M. Rosenthal, Y. I. Odarchenko, D. A. Ivanov, J. Feijen, and P. J. Dijkstra, Polymer **53**, 4033–4044 (2012).
19. L. Franco and J. A. Subirana, Synthesis **9297**, 3912–3924 (1998).
20. E. Armelin, C. Alemán, and J. Puiggali, J. Organ. Chem. **66**, 8076–8085 (2001).
21. Y. Chatani, Y. Ueda, H. Tadokoro, W. Deits, and O. Vogl, Macromolecules **11**, 636–638 (1978).
22. M. Cesari, G. Perego, and A. Mazzei, Makromolek. Chem. **83**, 196–206 (1965).
23. S. Lee and P. Phillips, Eur. Polym. J. **43**, 1933–1951 (2007).